The Astrophysical Journal, 584:1063–1070, 2003 February 20

SOLAR ENERGETIC PARTICLE PRODUCTION BY CORONAL MASS EJECTION–DRIVEN SHOCKS IN SOLAR FAST-WIND REGIONS

S. W. Kahler
Air Force Research Laboratory, Space Vehicles Directorate, 29 Randolph Road, Hanscom Air Force Base, MA 01731; stephen.kahler@hanscom.af.mil

and

D. V. Reames
NASA Goddard Space Flight Center, Greenbelt, MD 20771
Received 2002 September 10; accepted 2002 October 25

ABSTRACT

Gradual solar energetic particle (SEP) events at 1 AU are produced by coronal/interplanetary shocks driven by coronal mass ejections (CMEs). Fast ($v_{CME} \gtrsim 900$ km s^{-1}) CMEs might produce stronger shocks in solar slow-wind regions, where the flow and fast-mode MHD wave speeds are low, than in fast-wind regions, where those speeds are much higher. At 1 AU the O^{+7}/O^{+6} ratios distinguish between those two kinds of wind streams. We use the 20 MeV proton event intensities from the EPACT instrument on *Wind*, the associated CMEs observed with the LASCO coronagraph on *SOHO*, and the *ACE* SWICS solar wind values of O^{+7}/O^{+6} to look for variations of peak SEP intensities as a function of O^{+7}/O^{+6}. No significant dependence of the SEP intensities on O^{+7}/O^{+6} is found for either poorly connected or well-connected CME source regions or for different CME speed ranges. However, in the 3 yr study period we find only five cases of SEP events in fast wind, defined by regions of $O^{+7}/O^{+6} < 0.15$. We suggest that in coronal holes SEP acceleration may take place only in the plume regions, where the flow and Alfvén speeds are low. A broad range of angular widths are associated with fast ($v_{CME} \geq 900$ km s^{-1}) CMEs, but we find that no fast CMEs with widths less than 60° are associated with SEP events. On the other hand, nearly all fast halo CMEs are associated with SEP events. Thus, the CME widths are more important in SEP production than previously thought, but the speed of the solar wind source regions in which SEPs are produced may not be a factor.

Subject headings: solar wind — Sun: coronal mass ejections (CMEs) — Sun: particle emission

1. INTRODUCTION

Gradual solar energetic particle (SEP) events at 1 AU are understood to originate in coronal and interplanetary shocks driven by fast ($v_{CME} \gtrsim 700$ km s^{-1}) coronal mass ejections (CMEs; Reames 1999; Kahler 2001). In these SEP events a general correlation between the logs of the peak SEP intensities I and the logs of v_{CME} of the associated CMEs is found (e.g., Kahler 2001). In these correlations, however, a considerable scatter of about 4 orders of magnitude in the peak SEP intensities corresponding to a given CME speed range is also found. This suggests that while the speed of the CME driving the shock is an important factor in determining the resulting peak SEP intensity, other significant factors are involved.

Kahler (2001) investigated two such candidate factors, the variations of energy spectra among SEP events and the presence of enhanced ambient SEP intensities. In the first case, comparing $E > 10$ MeV and $E > 60$ MeV peak intensities of SEP events observed with the *GOES* spacecraft, he found that the spectral variations accounted for at least 1 of the 4 orders of magnitude in the $\log I / \log v_{CME}$ variation. If a perfect correlation between $\log v_{CME}$ and $\log I$ were found at one energy, 10 MeV for example, then for 60 MeV the peak intensities of the events would range over at least an order of magnitude at a given value of v_{CME}. In addition, correlations were also found between logs of peak SEP intensities and logs of ambient, i.e., pre-event, SEP intensities. This result would be expected if the enhanced ambient SEPs served as seed particles for CME-driven shocks, effectively making those shocks more efficient than shocks operating only on thermal coronal and solar wind material.

We now consider another factor that may play an important role in determining whether or how efficiently fast CMEs can drive shocks that accelerate ions. That factor is the variation of the CME speeds required to drive shocks in different coronal regions. The corona supports two kinds of solar wind flows, the fast wind that arises along the open magnetic fields of coronal holes (CHs) and the slow wind that arises at boundaries of CHs and over closed field structures (Wang et al. 1996; Schwadron, Fisk, & Zurbuchen 1999; Posner et al. 2001). The characteristic widths of CMEs are ~60° (St. Cyr et al. 2000) and typically extend over several kinds of coronal source regions (Subramanian et al. 1999).

Several observational results suggest that SEP acceleration is limited to the slow wind near the Sun. The first is that kilometric type II radio bursts, resulting from CME-driven shocks, lie predominately in high-density regions characteristic of the slow wind (Reiner et al. 1998). The second is that abundance enhancements of elements with low first ionization potential (FIP) are larger in SEPs than in energetic particles produced in corotating interaction region (CIR) reverse shocks (Reames, Richardson, & Barbier 1991; Fränz et al. 1999; Reames 2001). The reverse shocks are produced in the fast-wind streams by the flow of fast streams into preceding slow streams, and they accelerate particles out of only the fast streams. The generally lower enhancements of low-FIP elements in those energetic particles accelerated

from fast streams contrast with the more highly enhanced low-FIP abundances of SEP populations.

1.1. *Characteristic Speeds in the Solar Minimum Corona*

To produce a shock, the CME driving through the ambient solar wind must satisfy the condition $v_{\rm CME} > v_{\rm flow} + v_{\rm fast}$, where $v_{\rm flow}$ is the solar wind flow speed and $v_{\rm fast}$ is the solar wind MHD fast-mode speed in the solar wind frame along the line of propagation of the CME. For the corona we can take $v_{\rm fast} \approx (v_{\rm A}^2 + c_s^2)^{1/2}$ (Wang, Lean, & Sheeley 2000), where $v_{\rm A}$ is the Alfvén speed and c_s is the sound speed. In the corona $c_s \approx 170$ km s^{-1} (Lang 1974).

Height profiles of $v_{\rm flow}$ have been deduced for the polar CH fast-wind regions from the Ultraviolet Coronagraph Spectrometer (UVCS) on the *Solar and Heliospheric Observatory* (*SOHO*) by Kohl et al. (1998) and Li et al. (1998). Coronal slow-wind speed profiles have been derived from UVCS streamer-belt observations (Strachan et al. 2002) and from observations of white-light blobs that originate at about 3–4 $R_\odot$ (Sheeley et al. 1997). These observations show that within 10 $R_\odot$ the fast-wind flow speeds exceed those of the slow wind, although the scatter in the latter values and the model dependence of the former make direct comparisons difficult. We can also appeal to the semiempirical models of Sittler & Guhathakurta (1999a, 1999b), which show that in the fast-wind region over the poles the flow speed can exceed 400 km s^{-1}, while in the equatorial plane the flow speeds are less than 100 km s^{-1} at 4 $R_\odot$. Figure 1*a*, reproduced from Guhathakurta, Sittler, & McComas (1999), makes clear the strong difference of speed profiles for the two limiting cases. Qualitatively similar results are seen in the coronal models of Wang et al. (1998, their Fig. 6) and of Suess et al. (1999, their Fig. 4).

The determination of $v_{\rm fast}$ is made difficult by the lack of coronal magnetic field measurements. Here again we appeal to coronal models that show explicitly the spatial distributions of either the Alfvén speed $v_{\rm A}$ or the plasma β. Since $\beta \sim 2(c_s/v_{\rm A})^2$, we see that we can estimate the variation in $v_{\rm fast}$ from any given variation in β if we assume that variations in the temperature between the fast and slow wind are minimal and that $c_s \approx 170$ km s^{-1} throughout the corona. Various models showing the spatial variations of β from polar CH to equatorial streamer (e.g., Fig. 1*c* of Sittler & Guhathakurta 1999a, Fig. 11*a* of Sittler & Guhathakurta 1999b, Fig. 2 of Suess & Nerney 2002, and Fig. 5*b* of Wang et al. 1998) consistently show β ranging from $\sim 10^{-2}$ in the polar region to $\gtrsim 3$ in streamers. Suess et al. (1999) found $\beta > 1$ everywhere above 1.5 $R_\odot$ in their model streamer, and Gary (2001) has pointed out that in active regions $\beta > 1$ above ~ 1.2 $R_\odot$. Assuming a nominal value of $c_s = 170$ km s^{-1} and taking values of β more typical of 2–10 $R_\odot$, these results suggest that $v_{\rm fast}$ ranges from $\gtrsim 5000$ km s^{-1} in CHs to $\lesssim 300$ km s^{-1} in streamers and above active regions, consistent with the plots of $v_{\rm A}$ of Figure 1.

Combining $v_{\rm fast}$ and $v_{\rm flow}$ to determine the required CME speeds to drive shocks, we estimate that they range from $\lesssim 500$ km s^{-1} in streamers to $\gtrsim 5000$ km s^{-1} outside streamer regions. We therefore would expect that at least in the region 1.5–10 $R_\odot$, where SEP acceleration and injection begins (Kahler 1994), shock formation and SEP production would be confined to slow-wind regions, except for the exceptionally fast ($v_{\rm CME} \gtrsim 2000$ km s^{-1}) CMEs. Another possibility is that while shocks form in both solar wind regions, they have higher Mach numbers and compression ratios in the slow wind, resulting in harder SEP energy spectra (Jones & Ellison 1991).

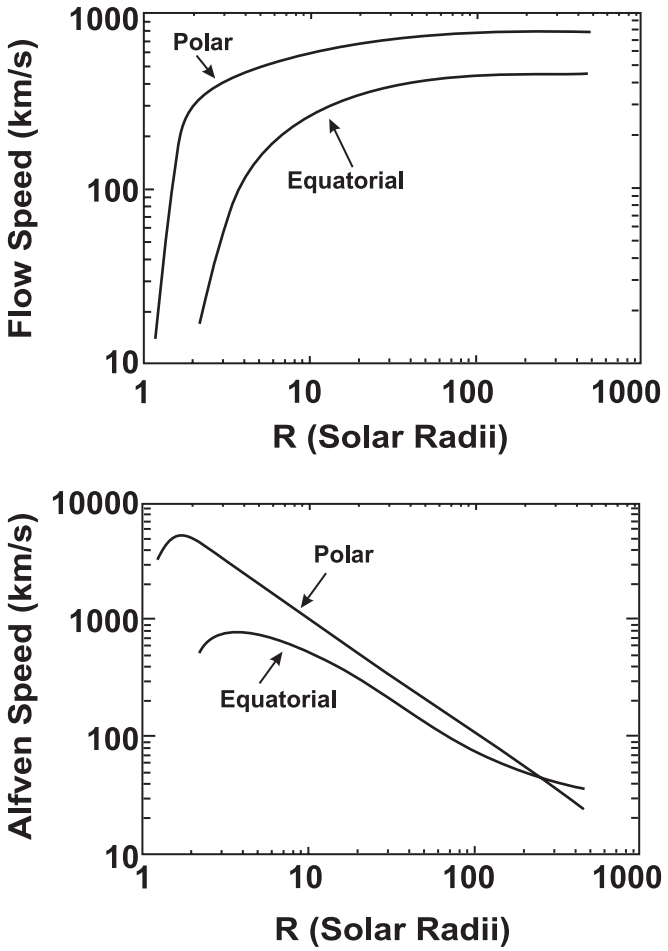

FIG. 1.—Plots of flow speeds (*top*) and $v_{\rm A}$ (*bottom*) for polar and equatorial sources of the fast and slow wind, respectively. Adapted from the semiempirical model of Guhathakurta et al. (1999).

1.2. *The* O^{+7}/O^{+6} *Solar Wind Signature*

The boundaries between the slow and fast solar winds during the first southern polar pass of the *Ulysses* spacecraft were distinguished by relatively sharp spatial boundaries of the values of O^{+7}/O^{+6}, Mg/O, and Fe/O in the SWICS instrument (Geiss et al. 1995). The ratio O^{+7}/O^{+6}, in particular, implied freeze-in temperatures of either ~ 1.6 MK in a slow wind or ~ 1.3 MK in a fast wind. The corresponding wind-speed profiles at the boundaries were much more gradual, having been washed out by stream-stream dynamics. Longer time averages of the *Ulysses* O^{+7}/O^{+6} observations showed a simple low-temperature freezing-in process for the fast wind but a more complicated range of high charge states for the slow wind (von Steiger et al. 2000).

The O^{+7}/O^{+6} ratios have also been examined in transient solar wind flows. A study of 56 interplanetary CMEs (ICMEs) observed with the *Ulysses* spacecraft showed that the ratios in ICMEs with magnetic cloud structures were enhanced, while ratios in ICMEs without cloud structures were usually unchanged in comparison to the ambient solar wind (Henke et al. 2001). In a more limited study of ICMEs

with observations from the *ACE* spacecraft Burlaga et al. (2001) found $O^{+7}/O^{+6} > 1$ for all four magnetic clouds and >0.7 for four of the five complex ejecta. These results show that the O^{+7}/O^{+6} signatures of transient flows either match those of the surrounding corotating wind streams or are enhanced, reflecting solar sources similar to the those of the slow wind.

1.3. *Characteristic Speeds and the* O^{+7}/O^{+6} *Signature at Solar Maximum*

We have to be careful in extending the observations and models of CHs at solar minimum to the conditions near solar maximum, which characterize the observations of this study. Miralles et al. (2001) found that the O^{+5} outflow velocities below 3 $R_\odot$ in a large equatorial CH observed in 1999 were 3–4 times lower than those of the polar CHs at solar minimum, although the associated wind speeds at 1 AU were comparable to within ~15% of those at solar minimum. Thus, for high-speed streams at solar maximum it appears that $v_{\rm flow}$ in the low corona is significantly lower than at solar minimum, but must reach comparable values at some point in the acceleration region, which is not presently clear.

The variation of $v_{\rm fast}$ between the polar CHs at solar maximum and the equatorial CHs at solar minimum should be small. Since $v_{\rm A}^2$ scales as B^2/n_e, the basic question is how B and n_e vary between the polar and equatorial CHs. The modeling analysis of Miralles et al. (2001) indicated that the density n_e of the 1999 equatorial CH was several times larger than that of the polar CHs. As Wang et al. (2000) note, the fraction of the Sun's surface covered by CHs is ~4 times larger at solar minimum than at solar maximum, while the average CH field is ~4 times larger at solar maximum than at solar minimum. Thus, the larger fields and densities should result in at least comparable values of $v_{\rm A}$ and $v_{\rm fast}$ for the equatorial CHs. The result is that the large disparity in $v_{\rm fast}$ between coronal slow-wind and fast-wind sources can be expected to exist during solar maximum as well as at solar minimum.

The O^{+7}/O^{+6} ratios have been examined in several *Ulysses* comparative studies of fast-wind streams at solar maximum and minimum. McComas, Elliot, & von Steiger (2002) examined nine high-latitude fast-wind streams from CHs in 2000–2001 and found low O^{+7}/O^{+6} temperatures at the peaks of the streams comparable to those found for the faster high-speed streams at solar minimum. Zurbuchen et al. (2002) found that the bimodal speed and O^{+7}/O^{+6} distributions of the first *Ulysses* orbit at solar minimum were replaced by single-peaked distributions during comparable times of the second orbit at solar maximum. However, the elemental composition observed when $O^{+7}/O^{+6} < 0.1$ had a relative enhancement of the elements with low FIP of only 1.82, characteristic of high-speed wind and significantly lower than that of 2.57, observed when $O^{+7}/O^{+6} > 0.1$. In a study of four solar rotations during the 1998–2001 period Neugebauer et al. (2002) also found that solar wind mapping back to CHs had lower O^{+7}/O^{+6} ratios than solar wind that mapped back to active regions. These studies indicate that although the very low ($\lesssim 0.03$) O^{+7}/O^{+6} ratios defining high-speed streams at solar minimum are rarely observed at solar maximum, O^{+7}/O^{+6} ratios can still be used as markers of high-speed streams at solar maximum, particularly if $O^{+7}/O^{+6} < 0.1$.

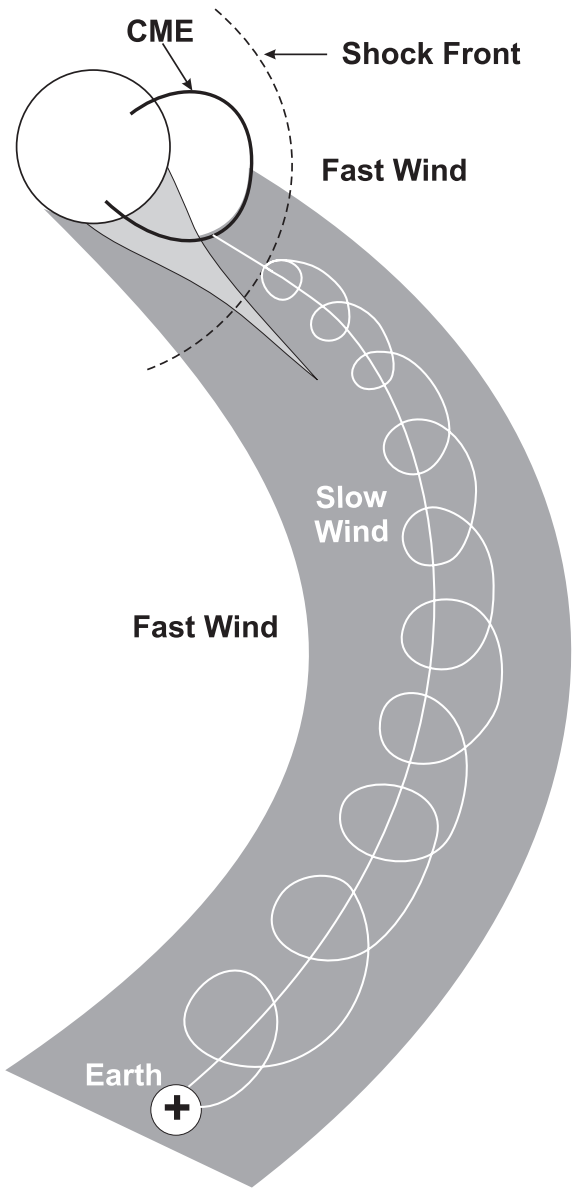

FIG. 2.—Cartoon showing the connection of a slow-wind region at 1 AU to the coronal source region with an embedded streamer. The CME extends over both slow- and fast-wind regions. Unless the CME speed $v_{\rm CME}$ is extremely fast, the preceding wave disturbance might be expected to produce a shock only in the slow-wind regions in which $v_{\rm flow} + v_{\rm fast} < v_{\rm CME}$.

We can test the proposition that fast-wind regions are less favorable for CME-driven shocks and consequent SEP events by asking whether we see more or larger SEP events from fast CMEs when the Earth lies in a slow-wind region. The O^{+7}/O^{+6} signature at 1 AU will be used to determine the type of solar wind, although we know from the *ACE* results (Zurbuchen et al. 2002) that we will not encounter the bimodal O^{+7}/O^{+6} distribution seen on the first orbit of *Ulysses*. The cartoon in Figure 2 shows that the solar wind region observed at 1 AU extends back to the corona, where the CME shock must accelerate the SEPs subsequently observed at 1 AU. Thus, any SEPs observed in a fast-wind stream must have been accelerated in that same stream near the Sun. A CME of a given speed may drive a shock in the slow-wind region, but not in the fast-wind region.

2. DATA ANALYSIS

We first selected from the Web page[1] maintained by the Catholic University all fast ($v_{CME} \geq 900$ km s^{-1} from linear height-time plots) CMEs with either western hemisphere position angles or halos observed by the Large Angle Spectroscopic Coronagraph (LASCO; Brueckner et al. 1995) on the *SOHO* spacecraft. The CME location criterion was chosen to optimize the solar magnetic connection of the Earth. In addition, we selected all CMEs associated with 20 MeV proton SEP events observed in the Energetic Particles: Acceleration, Composition, and Transport (EPACT; von Rosenvinge et al. 1995) instrument on *Wind*. The CME associations were made by comparing the timing and location of the CMEs with the onset times of the SEP events. Velocity dispersion between 2 and 20 MeV protons was used to select only prompt events and exclude shock or corotating SEP events. For each of the CMEs an attempt was made to determine the solar source region using Hα flare reports or movies from the EUV Imaging Telescope (EIT; Delaboudiniére et al. 1995) or the *Yohkoh* Soft X-Ray Telescope (SXT). When the CME source region could not be identified, the event was not used in the analysis.

The CME onset times were compared with the hourly values of the O^{+7}/O^{+6} ratios of the *ACE* SWICS (Solar Wind Ion Composition Spectrometer; Gloeckler et al. 1998) level 2 data.[2] Since the level 2 SWICS data are available only from 1998 January 23, we used the inclusive 3 yr period 1998–2000 for this study. The result was a selection of 118 CMEs. Many of those CMEs could not be associated with 20 MeV EPACT SEP events, but in a few cases the ambient SEP intensity was high at the time of the CME. We arbitrarily took 10^{-2} protons cm^{-2} s^{-1} sr^{-1} MeV^{-1} as an ambient intensity cutoff above which the SEP association of a CME was considered indeterminate. Eleven such cases reduced the CME sample to 107, with associated solar source longitudes ranging from the eastern hemisphere to just behind the west limb. For the purpose of plotting those cases of fast CMEs with no associated SEP events we set $I(20\ \text{MeV}) = 3 \times 10^{-4}$ protons cm^{-2} s^{-1} sr^{-1} MeV^{-1}, near the quiet-time background.

The direct propagation time of 20 MeV protons from the Sun to the Earth is $\lesssim 1$ hr, so each of the CME onset times was plotted on the corresponding Bartels 27 day plot of hourly averages of O^{+7}/O^{+6}, and the approximate value of O^{+7}/O^{+6} at the time of the CME was determined. An example is shown in Figure 3. We then plotted the logs of the peak 20 MeV SEP intensities I(20 MeV) against the associated logs of O^{+7}/O^{+6} to look for a correlation, which we might expect to be positive; i.e., a high value of O^{+7}/O^{+6}, indicating a slow solar wind, would be more likely to be associated with a larger I(20 MeV). We first selected all CMEs with solar source associations from W30° to behind the west limb, a total of 75 CMEs, as the population with a good magnetic connection to Earth and show the result in Figure 4. There is clearly no correlation in the plot, as indicated in Table 1. We then separated those CMEs into three groups: $900 \leq v_{CME} < 1000$ km s^{-1}, $1000 < v_{CME} < 1200$ km s^{-1}, and $v_{CME} \geq 1200$ km s^{-1}. We plotted values of $\log I(20\ \text{MeV})$ against $\log (O^{+7}/O^{+6})$ for each group to see whether the CMEs of lower speeds might show some correlation not present in the group of CMEs of faster speeds. As shown in Table 1, we found no significant correlation in any speed group.

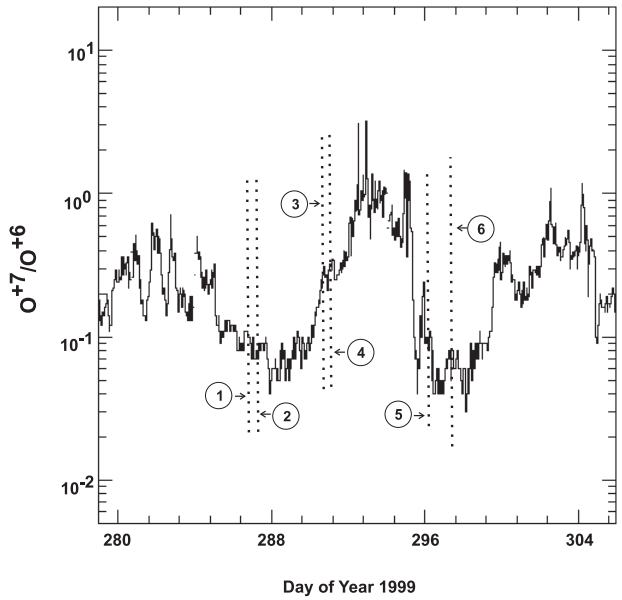

FIG. 3.—Example of the 27 day plot of hourly averages of O^{+7}/O^{+6} from the *ACE* SWICS experiment for Bartels rotation 2269. Superposed times of fast ($v \geq 900$ km s^{-1}) CMEs from the study are shown as vertical dotted lines. The numbers 1–6 correspond to the following 1999 CME dates and onset times: (1) October 13 at 21:06 UT, (2) October 14 at 09:26 UT, (3) October 18 at 02:06 UT, (4) October 18 at 14:26 UT, (5) October 23 at 01:26 UT, and (6) October 24 at 11:26 UT. Only CME 2 was associated with an SEP event.

Since most CMEs associated with SEP events appeared to have large angular widths, we plotted $\log I(20\ \text{MeV})$ against the CME widths, as shown in Figure 5. The narrowest CME associated with an SEP event had a width of 54°; that CME was associated with an impulsive Z-rich SEP

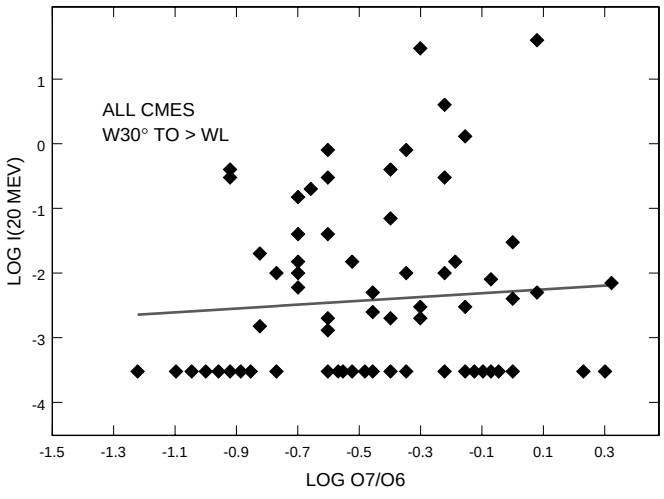

FIG. 4.—Plot of $\log I(20\ \text{MeV})$ vs. $\log (O^{+7}/O^{+6})$ for all CMEs of the study with source regions located from W30° to beyond the west limb. When no associated SEP event was found, $\log I(20\ \text{MeV})$ was set at -3.52 for the CME. The solid line is the least-squares best fit to the data.

[1] The site is located at http://cdaw.gsfc.nasa. gov/CME_list.

[2] Posted on the Web pagehttp://www.srl.caltech.edu/ACE/ASC/level2/lvl2DATA_SWICS_SWIMS.html.

TABLE 1
CORRELATION COEFFICIENTS (CC) AND PROBABILITIES (CP) OF PLOTS

CME Group	Plot	CMEs	CC	CP
W30° to WL	log I vs. CME width	75	0.597	>0.999
	log I vs. log (O^{+7}/O^{+6})	75	0.075	0.52
W30° to WL and $900 \leq v < 1000$ km s^{-1}	log I vs. log (O^{+7}/O^{+6})	31	0.067	0.72
W30° to WL and $1000 \leq v < 1200$ km s^{-1}	log I vs. log (O^{+7}/O^{+6})	20	0.132	0.58
W30° to WL and $v \geq 1200$ km s^{-1}	log I vs. log (O^{+7}/O^{+6})	24	0.125	0.56
Wide W30° to WL	log I vs. log (O^{+7}/O^{+6})	55	0.036	0.21
Wide W30° to WL and $900 \leq v < 1000$ km s^{-1}	log I vs. log (O^{+7}/O^{+6})	23	0.087	0.31
Wide W30° to WL and $1000 \leq v < 1200$ km s^{-1}	log I vs. log (O^{+7}/O^{+6})	14	0.160	0.42
Wide W30° to WL and $v \geq 1200$ km s^{-1}	log I vs. log (O^{+7}/O^{+6})	18	0.168	0.50
W46° to W90°	log I vs. log (O^{+7}/O^{+6})	50	0.045	0.24
Outside W46° to W90°	log I vs. log (O^{+7}/O^{+6})	57	0.128	0.65
SEP-associated from W46° to W90°	log I vs. log (O^{+7}/O^{+6})	28	0.170	0.61
	log R vs. log (O^{+7}/O^{+6})	25	0.201	0.64
SEP-associated outside W46° to W90°	log I vs. log (O^{+7}/O^{+6})	34	0.164	0.65
	log R vs. log (O^{+7}/O^{+6})	33	0.190	0.71

event on 2000 May 1 (Kahler, Reames, & Sheeley 2001) and was therefore not a proper gradual SEP event, although we have treated it as such here. All 20 CMEs narrower than 54° were not associated with SEP events. If we count the May 1 event as not associated with an SEP event, then all 23 CMEs narrower than 60° are not SEP-associated. On the other hand, only two of the 16 halo (360°) events were not SEP-associated. This suggests that CME width is an important parameter in understanding the association between fast CMEs and SEP events.

We deleted the 20 narrow (<54°) CMEs and calculated the log I(20 MeV) versus log (O^{+7}/O^{+6}) correlations for the remaining 55 CMEs and for the individual speed groups, but the results, shown in Table 1, were similar to those with the narrow CMEs. As a final test for any correlation between log I(20 MeV) and log (O^{+7}/O^{+6}), we divided all the CMEs between a group of 50 CMEs with well-connected source regions of W46°–W90° and a group of 57 CMEs with poorly-connected source regions of all remaining longitudes. The non-SEP CMEs were removed from each group and correlation coefficients were again calculated. The results, given in Table 1, show once again that no correlation is found between log I(20 MeV) and log (O^{+7}/O^{+6}) for any of these CME groups.

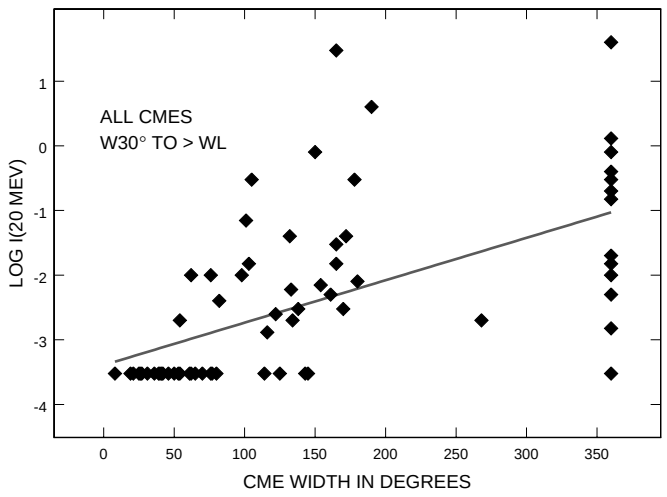

FIG. 5.—Plot of log I(20 MeV) vs. CME width for the 75 CMEs with solar source associations from W30° to behind the west limb. Of the 23 CMEs with widths less than 60° only one, on 2000 May 1, was associated with an SEP event, which was an impulsive SEP event. The halo events are the points at 360°. The diagonal line is the least-squares best fit to the data.

To confirm that we had clear cases of fast CMEs with the Earth in fast-wind regions, we have listed all such cases in Table 2, in which we have considered all 107 CMEs of the sample except for the 23 CMEs not wider than 60°. We take $O^{+7}/O^{+6} < 0.15$ (T. Zurbuchen 2002, private communication) to indicate fast-wind regions. The time of first appearance and the speed of the CME are given in the second and third columns. In addition, we separately examined the *ACE* solar wind parameters to select periods that were clearly fast-wind streams based on peak speeds greater than 500 km s^{-1}, low electron densities and magnetic-field intensities, and enhanced proton temperatures. The selected periods of fast-wind streams generally coincided with low values of O^{+7}/O^{+6}. Whether the Earth was in one of the selected periods of fast-wind streams at the time of a fast CME is given in the last column of Table 2. The table entries are ordered by longitude, with the last three behind the west limb. The three events of 1999 October, one of which was a SEP event, are indicated in Figure 3 as event numbers 2, 5, and 6.

Five of the 11 CMEs of Table 2 were associated with SEP events; upper limits to the 20 MeV SEP intensities are given for the six others. Three of the five CMEs with SEP events appeared in solar wind with clear fast-wind signatures. To determine whether higher CME speeds might be required to produce SEP events in the fast-wind streams, we compare the 11 events of Table 2 with those of the remaining 73 CMEs for which $O^{+7}/O^{+6} \geq 0.15$. For the latter group, the median speed of the 56 CMEs with SEP events was 1103 km s^{-1} and for the 17 CMEs without SEP events 1017 km s^{-1}. For the CMEs of Table 2 the median speed of the five CMEs with SEP events was 1336 km s^{-1} and for the six CMEs without SEP events, 1070 km s^{-1}. Comparing the 11 CMEs of Table 2 with the remaining 73 CMEs, we therefore find that fast CMEs in fast-wind regions are less likely to be associated with SEP events and if associated, have higher CME speeds. However, the limited numbers of events in Table 2 obviously preclude a definitive conclusion on these associations.

TABLE 2
FAST AND WIDE (>60°) CMEs IN REGIONS OF $O^{+7}/O^{+6} < 0.15$

CME Date	Time (UT)	Speed (km s^{-1})	Source Region	I(20 MeV) (protons cm^{-2} s^{-1} sr^{-1} MeV^{-1})	O^{+7}/O^{+6}	Fast Wind?
1999 May 3	06:06	1584	N15°E32°	0.02	0.14	Yes
1999 Oct 14	09:26	1250	N11°E32°	0.0015	0.09	No
2000 Feb 8.....	09:30	1079	N25°E26°	<3(−4)	0.13	No
2000 Nov 24...	15:30	1245	N22°W07°	1.5	0.095	No
1999 Aug 28 ...	01:26	1147	S26°W16°	<3(−4)	0.10	Yes
2000 Jan 28	20:12	1177	S31°W17°	<3(−4)	0.06	Yes
1998 May 9	03:35	2331	S11°W90°	0.3	0.12	Yes
1999 Oct 23	01:26	1012	W90°	<2(−4)	0.10	Yes
1999 Oct 24	11:26	1127	NW limb[a]	<5(−4)	0.06	Yes
2000 Jun 17	23:10	927	W limb[a]	<3(−4)	0.11	No
2000 Oct 16	07:27	1336	W limb[a]	0.4	0.12	Yes

[a] Behind the west limb.

To look for any spectral differences among the SEP events that could be attributed to solar wind variations, we compared $\log R$ with $\log (O^{+7}/O^{+6})$, where $R = I(2\ \mathrm{MeV})/I(20\ \mathrm{MeV})$. In some cases it was not possible to determine an event value for I(2 MeV) because of high ambient 2 MeV intensities. We did the comparisons for the well-connected and poorly connected source regions, with the plot of the well-connected regions of W46° to W90° shown in Figure 6. The correlation was weakly positive, but insignificant in both cases. Since we might expect steeper SEP spectra to be associated with lower compression ratios of fast-wind regions, hence with lower values of O^{+7}/O^{+6}, the weak correlations are in the opposite sense of that expected.

3. DISCUSSION

3.1. *SEP Production in Fast Wind Regions*

In the basic paradigm of gradual SEP production (Reames 1999; Kahler 2001) SEPs are accelerated in coronal/interplanetary shocks driven by fast CMEs. A basic assumption is that the shock traverses the corona and interplanetary medium ahead of the leading edge of the CME.

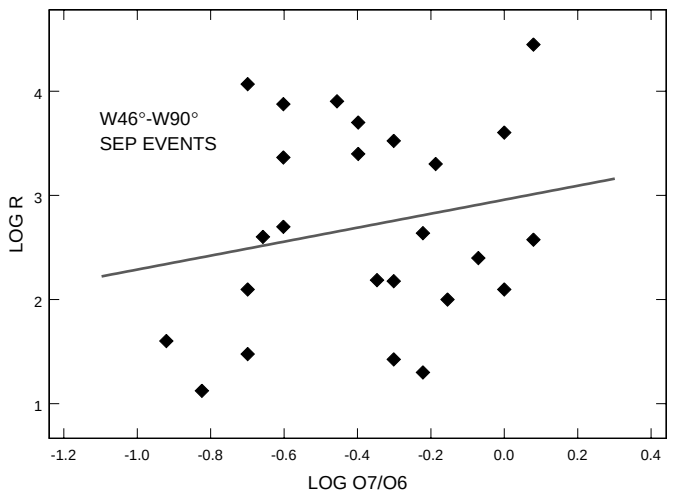

FIG. 6.—Plot of $\log R$ vs. $\log (O^{+7}/O^{+6})$ for well-connected SEP events, where $R = I(2\ \mathrm{MeV})/I(20\ \mathrm{MeV})$. The diagonal line is the least-squares best fit.

Coronagraph observations of the effects on streamers and raylike features of disturbances propagating away from fast CMEs (Sheeley, Hakala, & Wang 2000) appears consistent with this view. The measured disturbance speeds were also faster than the nominal MHD speeds in those regions, implying that they were shock waves. We expect that the CME-driven disturbances will propagate throughout the surrounding corona, forming shocks wherever the disturbance speed exceeds $v_{\mathrm{flow}} + v_{\mathrm{fast}}$.

The question we ask here is whether the CME-driven disturbances can form shocks and accelerate SEPs above CH regions that form the sources of fast-wind streams. Because $v_{\mathrm{flow}} + v_{\mathrm{fast}}$ is expected to be characteristically much higher in those regions than in the streamers and edges of CHs forming the sources of the slow wind, we should expect that shocks and SEPs are produced above CHs only by exceptionally fast CMEs. The five cases of SEP events occurring in fast-wind regions defined by $O^{+7}/O^{+6} < 0.15$ (Table 2) are consistent with the conclusion that faster CMEs are required to produce SEPs in fast-wind regions than in slow-wind regions. Furthermore, if we adopt a stricter fast-wind criterion of $O^{+7}/O^{+6} < 0.1$ (Zurbuchen et al. 2002), then we have only two qualifying SEP events, neither of which occurred in a clear fast-wind region, as defined by other solar wind parameters. In that case the confirmation of the existence of SEP events in the fast wind would have to be considered marginal. Because of the small sample size involved here, we have only weak evidence that faster CMEs are required to produce SEPs in fast-wind streams.

If SEP production does occur in CH regions, then the SEP elemental composition would be expected to reflect that of the fast-wind streams, as it does in the energetic particles accelerated out of the fast-wind regions in CIR reverse shocks. Although no effort has been made specifically to examine the composition of gradual SEP events observed only in fast-wind streams, the average low-FIP enhancements of gradual SEP events are distinctly higher than those of the CIR shocks (Reames 1998).

In the solar corona the low-FIP enhancement over equatorial regions is about a factor of 4, while in polar CHs it is less than a factor of 2 (Feldman et al. 1998). However, polar CHs consist of relatively dense, magnetically unipolar plumes and less dense interplume regions, so it is important to distinguish between the two regimes. The low-FIP enhancement of the interplume regions is less than a factor

of 2 (Doschek et al. 1998), but the low-FIP enhancement of one polar plume observed by *Skylab* was up to a factor 10 (Widing & Feldman 1992). The plumes are about 1.3–1.8 times denser (with a lower v_A) than the interplume regions and fill a significant fraction of the CH volume (Cranmer et al. 1999). However, Giordano et al. (2000) used observations with the *SOHO* UVCS to establish that the interplume regions are the dominant source of the fast solar wind, with expansion rates at 1.7 $R_\odot$ of 105–150 km s^{-1}, compared to only 0–65 km s^{-1} for the plumes. Of relevance to coronal shock formation is the observation in plumes of propagating wave disturbances with speeds of 300–500 km s^{-1}, near the estimated v_A (DeForest et al. 1997). Polar plumes are also observed to expand with a superradial expansion factor of $\sim$6 at 15 $R_\odot$ (DeForest et al. 1997) and are observed in the fast wind as pressure-balance structures (PBSs; e.g., Yamauchi, Suess, & Sakurai 2002). While these results are based on observations in polar CHs at solar minimum, Wang & Sheeley (1995) concluded that plumes may occur in open magnetic regions at any latitude.

We suggest that shock formation and SEP production in CHs and their fast-wind extensions into space occur only in coronal plumes. The low values of both $v_{\rm flow}$ and $v_{\rm fast}$ that characterize coronal plumes make them favorable sites for the required shock formation. While definitive measurements of the plume low-FIP enhancements remain to be made, the sparse evidence suggests that plume low-FIP enhancements, like those of the slow-wind source regions, exceed those of the interplume regions. The superradial expansions and large coronal volumes of plumes suggest a broad range of injection regions of shock-accelerated SEPs from plumes. With the low frequency f^{-1} turbulent spectrum in fast-wind regions (Goldstein et al. 1995) further suggesting supra-diffusive spreading of the CH magnetic field lines with solar distance (Ragot & Kirk 1997; Ragot 2001), fluctuations in the subsequent SEP temporal profiles at 1 AU might well be minimized.

The energetic ions produced in CIR shocks are drawn from interplume flows in the fast-wind regions with small enhancements ($\sim$2) of low-FIP elements. Thus, in our suggested scenario for fast-wind regions both the CIR energetic particles with small low-FIP enhancements and the gradual SEPs with large low-FIP enhancements originate in solar CHs, but they originate in different structural elements of the CHs.

Although we argued to the contrary in § 1.3, it may be the case that conditions for shock production in equatorial CHs, dominant during the 1998–2000 period of our investigation, are much more favorable than in the polar CHs, dominant at solar minimum. There is perhaps some evidence for this in the fact that SEP events were almost absent at the *Ulysses* spacecraft during its polar passage at solar minimum. In one case an intense SEP event on 1994 February 20 was observed at Earth, followed by the passage of the transient ejecta (Cane, Richardson, & von Rosenvinge 1996). The ejecta, a magnetic cloud, was also observed in the high-speed wind at *Ulysses*, located at S54° and 3.5 AU, but was accompanied by an SEP event orders of magnitude weaker (Bothmer et al. 1995). The magnetic cloud produced a forward and a reverse shock, and the SEPs were mostly confined within the cloud itself. Thus, an alternative possibility is that shocks are extremely difficult to produce in polar CHs, but CMEs are very infrequent at the time when the polar CHs are fully developed, so occasions when a fast CME occurs and an observer is located in a fast wind from a polar CH are rare.

3.2. *Narrow Fast CMEs*

The result that all 23 narrow (width <60°) fast CMEs were not associated with gradual 20 MeV SEP events suggests an intrinsic limitation of the ability of those narrow CMEs to drive the shocks that accelerate SEPs. Such a limitation was suggested in the result of Gopalswamy et al. (2001) that only 6 of 101 CMEs associated with decametric-hectometric (DH) type II radio bursts, attributed to coronal/interplanetary shocks, were narrower than 60°. Further, the average width of 142 fast ($v > 900$ km s^{-1}) CMEs limited to widths <200° and not associated with DH type II bursts was only 66°. Thus, while we found many fast, narrow CMEs not associated with gradual SEP events, Gopalswamy et al. (2001) also found a large population of fast, narrow CMEs unassociated with DH type II bursts.

The reason that narrow CMEs are ineffective in driving shocks is not clear. One possibility is that significant lateral expansion of CMEs is required to drive perpendicular shocks into adjacent radial magnetic fields. More than half of the CMEs associated with the DH shocks of the Gopalswamy et al. (2001) study were halo CMEs. This was true even for limb events, indicating rapid azimuthal expansion for those CMEs. St. Cyr et al. (1999) examined the angular widths of CMEs observed in both the Mauna Loa Mark III coronameter and the *Solar Maximum Mission* (*SMM*) coronagraph. Their result was that CMEs expand by an average 12° from the 1.15–2.4 $R_\odot$ field of view of the Mauna Loa coronameter to the 1.7– 6 $R_\odot$ field of view of the *SMM* coronagraph, but they did not attempt to distinguish among CMEs of different speeds and widths. We suggest that a more detailed study to compare CME expansion rates with shock formation may prove useful.

4. CONCLUSIONS

We have argued that the high value of $v_{\rm flow} + v_{\rm fast}$ expected in coronal fast-wind regions should result in fewer or weaker CME-driven shocks arising in those regions, with the result that fast-wind regions, with low O^{+7}/O^{+6} ratios, should show at 1 AU either a significant deficit in gradual SEP events or steeper SEP spectra compared with those of the slow-wind regions. Neither of these predictions was confirmed, suggesting that the shocks required to produce SEPs arise in both kinds of solar wind. A small sample of fast CMEs in confirmed fast-wind streams provided weak evidence that higher CME speeds may be required to produce shocks and SEPs in those streams. However, we do not have enough events to provide solid evidence regarding shock formation and SEP production in this type of solar wind. We suggest that polar plumes are CH regions of low $v_{\rm flow} + v_{\rm fast}$ in which CMEs can drive shocks and accelerate SEPs. They appear to have elemental abundances with large low-FIP enhancements without contributing significantly to the fast-wind flow observed at 1 AU.

The study included a comprehensive sample of fast ($v_{\rm CME} \geq 900$ km s^{-1}) CMEs of which we find that all 23 with widths less than 60° are not associated with gradual SEP events. This suggests that some property of the narrow CMEs makes them unsuitable for producing the shocks to accelerate SEPs.

We acknowledge extensive use of the LASCO CME catalog. This CME catalog is generated and maintained by the Center for Solar Physics and Space Weather, the Catholic University of America, in cooperation with the Naval Research Laboratory and NASA. *SOHO* is a project of international cooperation between ESA and NASA. We also acknowledge use of the *ACE* SWICS level 2 data posted on the *ACE* Web page. We thank N. Sheeley, Jr., and Y.-M. Wang for useful comments on the manuscript.

REFERENCES

Bothmer, V., Marsden, R. G., Sanderson, T. R., Trattner, K. J., Wenzel, K.-P., Balogh, A., Forsyth, R. J., & Goldstein, B. E. 1995, Geophys. Res. Lett., 22, 3369
Brueckner, G. E., et al. 1995, Sol. Phys., 162, 357
Burlaga, L. F., Skoug, R. M., Smith, C. W., Webb, D. F., Zurbuchen, T. H., & Reinard, A. 2001, J. Geophys. Res., 106, 20957
Cane, H. V., Richardson, I. G., & von Rosenvinge, T. T. 1996, J. Geophys. Res., 101, 21561
Cranmer, S. R., et al. 1999, ApJ, 511, 481
DeForest, C. E., Hoeksema, J. T., Gurman, J. B., Thompson, B. J., Plunkett, S. P., Howard, R., Harrison, R. C., & Hassler, D. M. 1997, Sol. Phys., 175, 393
Delaboudinière, J.-P., et al. 1995, Sol. Phys., 162, 291
Doschek, G. A., Laming, J. M., Feldman, U., Wilhelm, K., LeMaire, P., Schühle, U., & Hassler, D. M. 1998, ApJ, 504, 573
Feldman, U., Schühle, U., Widing, K. G., & Laming, J. M. 1998, ApJ, 505, 999
Fränz, M., Keppler, E., Lauth, U., Reuss, M. K., Mason, G.M., & Mazur, J. E. 1999, Geophys. Res. Lett., 26, 17
Gary, G. A. 2001, Sol. Phys., 203, 71
Geiss, J., et al. 1995, Science, 268, 1033
Giordano, S., Antonucci, E., Noci, G., Romoli, M., & Kohl, J. L. 2000, ApJ, 531, L79
Gloeckler, G., et al. 1998, Space Sci. Rev., 86, 495
Goldstein, B. E., Smith, E. J., Balogh, A., Horbury, T. S., Goldstein, M. L., & Roberts, D. A. 1995, Geophys. Res. Lett., 22, 3393
Gopalswamy, N., Yashiro, S., Kaiser, M. L., Howard, R. A., & Bougeret, J.-L. 2001, J. Geophys. Res., 106, 29219
Guhathakurta, M., Sittler, E. C., & McComas, D. 1999, Space Sci. Rev., 87, 199
Henke, T., Woch, J., Schwenn, R., Mall, U., Gloeckler, G., von Steiger, R., Forsyth, R. J., & Balogh, A. 2001, J. Geophys. Res., 106, 10597
Jones, F. C., & Ellison, D. C. 1991, Space Sci. Rev., 58, 259
Kahler, S. 1994, ApJ, 428, 837
Kahler, S. W. 2001, J. Geophys. Res., 106, 20947
Kahler, S. W., Reames, D. V., & Sheeley, N. R., Jr. 2001, ApJ, 562, 558
Kohl, J. L., et al. 1998, ApJ, 501, L127
Lang, K. R. 1974, Astrophysical Formulae (New York: Springer)
Li, X., Habbal, S. R., Kohl, J. L., & Noci, G. 1998, ApJ, 501, L133
McComas, D. J., Elliot, H. A., & von Steiger, R. 2002, Geophys. Res. Lett., 29, 10.1029/2001GL013940
Miralles, M. P., Cranmer, S. R., Panasyuk, A. V., Romoli, M., & Kohl, J. L. 2001, ApJ, 549, L257
Neugebauer, M., Liewer, P. C., Smith, E. J., Skoug, R. M., & Zurbuchen, T. H. 2002, Geophys. Res. Lett., in press
Posner, A., Zurbuchen, T. H., Schwadron, N. A., Fisk, L. A., Gloeckler, G., Linker, J. A., Mikic, Z., & Riley, P. 2001, J. Geophys. Res., 106, 15869
Ragot, B. R. 2001, in Proc. 27th Intl. Cosmic Ray Conf. (Germany), 8, 3293
Ragot, B. R., & Kirk, J. G. 1997, A&A, 327, 432
Reames, D. V. 1998, Space Sci. Rev., 85, 327
———. 1999, Space Sci. Rev., 90, 413
———. 2001, in AIP Conf. Proc. 598, Solar and Galactic Composition, ed. R. F. Wimmer-Schweingruber (New York: AIP), 153
Reames, D. V., Richardson, I. G., & Barbier, L. M. 1991, ApJ, 382, L43
Reiner, M. J., Kaiser, M. L., Fainberg, J., & Stone, R. G. 1998, J. Geophys. Res., 103, 29651
Schwadron, N. A., Fisk, L. A., & Zurbuchen, T. H. 1999, ApJ, 521, 859
Sheeley, N. R., Jr., Hakala, W. N., & Wang, Y.-M. 2000, J. Geophys. Res., 105, 5081
Sheeley, N. R., Jr., et al. 1997, ApJ, 484, 472
Sittler, E., & Guhathakurta, M. 1999a, in AIP Conf. Proc. 471, Solar Wind Nine, 9th Intl. Solar Wind Conf., ed. S. R. Habbal, et al. (New York: AIP), 401
Sittler, E. C., Jr., & Guhathakurta, M. 1999b, ApJ, 523, 812
St. Cyr, O. C., Burkepile, J. T., Hundhausen, A. J., & Lecinski, A. R. 1999, J. Geophys. Res., 104, 12493
St. Cyr, O. C., et al. 2000, J. Geophys. Res., 105, 18169
Strachan, L., Suleiman, R., Panasyuk, A.V., Biesecker, D. A., & Kohl, J. L. 2002, ApJ, 571, 1008
Subramanian, P., Dere, K. P., Rich, N. B., & Howard, R. A. 1999, J. Geophys. Res., 104, 22321
Suess, S. T., & Nerney, S. F. 2002, ApJ, 565, 1275
Suess, S. T., Wang, A.-H., Wu, S. T., Poletto, G., & McComas, D. J. 1999, J. Geophys. Res., 104, 4697
von Rosenvinge, T. T., et al. 1995, Space Sci. Rev., 71, 155
von Steiger, R., et al. 2000, J. Geophys. Res., 105, 27217
Wang, A. H., Wu, S. T., Suess, S. T., & Poletto, G. 1998, J. Geophys. Res., 103, 1913
Wang, Y.-M., Hawley, S. H., & Sheeley, N. R., Jr. 1996, Science, 271, 464
Wang, Y.-M., Lean, J., & Sheeley, N.R., Jr. 2000, Geophys. Res. Lett., 27, 505
Wang, Y.-M., & Sheeley, N. R., Jr. 1995, ApJ, 446, L51
Widing, K. G., & Feldman, U. 1992, ApJ, 392, 715
Yamauchi, Y., Suess, S. T., & Sakurai, T. 2002, Geophys. Res. Lett., 29, 10.1029/2001GL013820
Zurbuchen, T. H., Fisk, L. A., Gloeckler, G., & von Steiger, R. 2002, Geophys. Res. Lett., 29, 10.1029/2001GL013946